

Extraction of photogenerated charge carriers by linearly increasing voltage in the case of Langevin recombination

G. Juška,¹ N. Nekrašas,¹ V. Valentinavičius,¹ P. Meredith,² and A. Pivrikas^{2,3,*}

¹*Department of Solid State Physics, Vilnius University, 10222 Vilnius, Lithuania*

²*Centre for Organic Photonics and Electronics, The University of Queensland, Brisbane, Queensland 4072, Australia*

³*Linz Institute for Organic Solar Cells (LIOS), Physical Chemistry, Johannes Kepler University, 4040 Linz, Austria*

(Received 19 July 2011; revised manuscript received 2 September 2011; published 14 October 2011)

Charge extraction by linearly increasing voltage (CELIV) is a powerful and widely used technique for studying charge transport physics, particularly in disordered systems such as organic semiconductors. In this article, we show that CELIV photocurrent transients are strongly dependent on experimental conditions, such as the light intensity and absorption profile. With this in mind, we introduce a universal correction factor that qualitatively extends previously derived CELIV equations, allowing carrier mobility to be estimated at various photogenerated carrier concentrations and, most importantly, photogeneration profiles. In addition, we demonstrate how the CELIV technique can be conveniently used to determine precisely the presence of Langevin bimolecular carrier recombination.

DOI: [10.1103/PhysRevB.84.155202](https://doi.org/10.1103/PhysRevB.84.155202)

PACS number(s): 72.20.Jv, 71.55.Jv, 72.80.Ng, 73.61.Jc

I. INTRODUCTION

The charge extraction by linearly increasing voltage (CELIV) technique has already been widely applied to study fundamental charge carrier properties, such as mobility and recombination in a wide range of disordered semiconductors.^{1,2} The main advantages of CELIV compared with the classical time-of-flight technique are its applicability to thin films, its suitability for materials with high conductivity, and its allowance of studying relaxation of photogenerated carrier mobility and concentration independently.³ However, as has already been shown, CELIV transients are strongly influenced by carrier concentration, recombination, and electric field.^{4,5} In particular, the light absorption profile has not yet been considered, even though the photogenerated carrier distribution in the film strongly influences extraction transients.^{6,7} Application of the current equations to all experimental cases might lead to misinterpretation of CELIV transients and incorrect estimates of key parameters. Therefore, to estimate charge carrier mobility and recombination correctly, it is important to understand the CELIV transient dependencies on experimental parameters, such as light absorption depth, intensity, and recombination rate. With this imperative in mind, we present a further development of the CELIV technique to extend the range of applicability of the method for nonequilibrium photogenerated carrier extraction in the case of Langevin bimolecular carrier recombination, which is typically observed in low-mobility materials.

II. THEORETICAL DERIVATIONS

The essence of the CELIV technique is the application of a linearly increasing voltage pulse to extract the photogenerated charge carriers from the film, while blocking contacts prevent additional carrier injection into the film from the electrodes. The basic relation used to calculate the carrier mobility using linearly increasing voltage for surface-generated carrier extraction through the film at low concentrations was first published in 1975.⁸ In 2000, the equations to estimate the

equilibrium carrier mobility from CELIV transients at low, as well as at high, carrier concentrations were described.^{9,10} Here, we derive the analytical equation for CELIV photocurrent transients at low photogenerated charge carrier concentrations when the extracted charge negligibly changes the distribution of the electric field. The time-dependent carrier drift velocity through the film under applied nonconstant bias can be written as

$$v(t) = \mu E(t) = \frac{At\mu}{d} = \frac{dl(t)}{dt}, \quad (1)$$

where μ is the mobility of the faster charge carriers ($\mu_{\text{faster}}/\mu_{\text{slower}} \gg 1$, which is typically observed in organic semiconductors), $E(t)$ is the electric field, A is the rate of the linearly increasing voltage pulse, d is the film thickness, and $l(t)$ is the extraction depth (the edge between the depletion region and mobile carriers). Solving Eq. (1), the transit time through the whole film thickness at low carrier concentrations can be obtained:⁸

$$t_{\text{tr}} = d \sqrt{\frac{2}{\mu A}} \quad (2)$$

The transit time, t_{tr} , defines the time a charge (under conditions of low concentration such that it does not significantly perturb the applied electric field) takes to move through the whole film thickness starting from the surface.

The time-dependent total current density is the sum of the current densities due to displacement charging and due to transported mobile charge carriers,

$$j(t) = \varepsilon \varepsilon_0 \frac{dE(x,t)}{dt} + e\mu p(x,t) E(x,t), \quad (3)$$

where ε and ε_0 are the relative and vacuum permittivities, respectively, and $p(x,t)$ is the concentration of faster carriers.

Equation (3) is solved by averaging it over coordinate x and noting that the conductivity of the depletion layer formed between $x = 0$ and $x = l(t)$ is negligible, with no fast carriers

present in said depletion region:

$$j(t) = \frac{\varepsilon\varepsilon_0 A}{d} + \frac{e\mu}{d} \int_{l(t)}^d p(x,t)E(x,t)dx. \quad (4)$$

Film thickness d and light absorption coefficient α (from the Beer–Lambert law) of the studied material determine the distribution of photogenerated charge carriers in the film, which influences the CELIV extraction transients. The initial coordinate-dependent distribution of carriers, $p(x, 0)$, photogenerated in the film due to the Beer–Lambert law by the short laser pulse prior to their extraction is:

$$p(x, 0) = L_0\alpha e^{-\alpha x}, \quad (5)$$

where L_0 is the light intensity per square unit multiplied by the quantum efficiency of charge carrier generation. Equation (4) can be solved analytically for low carrier concentration using Eqs. (1), (2), and (5),

$$j(t) = \frac{\varepsilon\varepsilon_0 A}{d} + \frac{eL_0}{d} (1 - e^{-\alpha d(1-t^2/t_{tr}^2)}) \frac{\mu A t}{d} = j_0 + \Delta j(t), \quad (6)$$

which can be further restructured,

$$\frac{\Delta j(t)}{j_0} = \frac{eL_0\mu}{\varepsilon\varepsilon_0 d} t (1 - e^{-\alpha d(1-t^2/t_{tr}^2)}), \quad (7)$$

where j_0 is the displacement current density. By taking the time derivative of Eq. (7) and setting it to zero, the extraction maximum time t_{\max} is found:

$$e^{-\alpha d(1-t_{\max}^2/t_{tr}^2)} (1 + 2\alpha d t_{\max}^2/t_{tr}^2) = 1. \quad (8)$$

It is important to emphasize that both Eq. (7) and Eq. (8) are derived for charge transport in the low-concentration regime, where bimolecular recombination is negligible. Nevertheless, Eqs. (7) and (8) do explicitly incorporate details of the light absorption profile, and they are very useful analytical expressions for interpreting CELIV transients.

III. NUMERICAL CALCULATIONS

The absence of a simple analytical expression for CELIV photocurrent transients at high carrier concentrations requires the transients be calculated numerically using a previously

published formalism based upon a numerical solution of the Poisson, continuity, and current equations.^{6,7} In the present calculations, the Langevin bimolecular carrier recombination with coefficient $\beta_L = e(\mu_{\text{faster}} + \mu_{\text{slower}})/\varepsilon\varepsilon_0$ is used. Carrier diffusion, trapping, light interference in thin films, as well as contact effects are not accounted for in the simulations. Numerical calculations that account for carrier diffusion show that the extraction maximum t_{\max} only shortens insignificantly when $\alpha d > 1$; therefore, for thin films, the influence of diffusion can be neglected.

Adopting such an approach, Fig. 1(a) shows the numerically calculated current density, $\Delta j(t)$, transients, which are normalized to the displacement current density step, j_0 , at high carrier concentration ($L = 100$ as an example). Here, L is the light intensity (in amount of incoming photons while assuming quantum efficiency for carrier generation is 1) normalized to the density of charge carriers in the electrode (charge that is determined by the device capacitance and applied voltage) at time $t = t_{tr}$. As can be seen, the current density at the extraction maximum (Δj_{\max}) does not exceed the displacement current density step (j_0) due to fast Langevin recombination. As expected, Fig. 1(a) demonstrates that CELIV transients indeed are strongly influenced by carrier distribution in the film, and this must be accounted for in order to correctly calculate carrier mobility from the extraction maximum, as is common practice.

From the numerically calculated CELIV current density transients t_{\max} was estimated at various photogenerated carrier concentrations (L) and light absorption profiles in the film (αd), as shown in Fig. 1(b). The t_{\max} is normalized to the transit time t_{tr} for small charge (Eq. (2)). At low carrier concentrations ($L < 1$), t_{\max} shifts to longer time scales when the carrier distribution becomes surface concentrated (αd increasing), since surface-generated charge carriers have to travel a longer distance prior to their extraction from the film. At high carrier concentrations ($L > 1$), t_{\max} slightly decreases when photogeneration changes from volume (small αd) to surface (large αd). This is attributed to the electric field redistribution and carrier recombination. Note, in the high αd limit, t_{\max} approaches and becomes equal to t_{tr} . In this case, Eq. (2) is used to calculate charge carrier mobility.

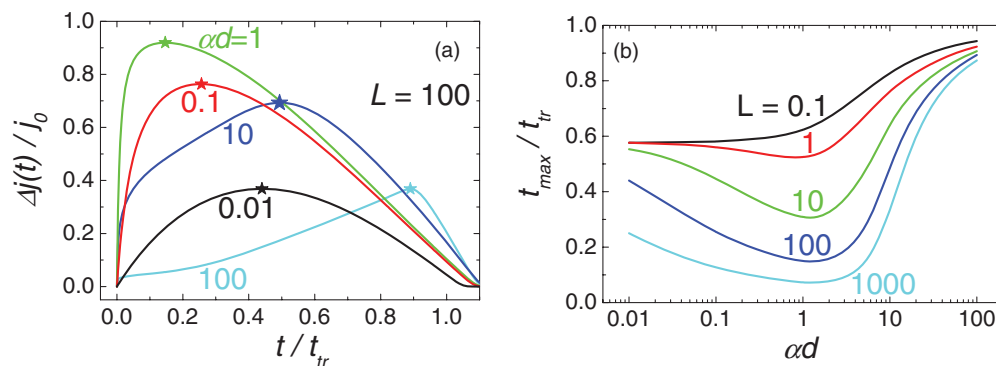


FIG. 1. (Color online) (a) Numerically calculated current transients $\Delta j(t)/j_0$ and (b) extraction maximum time t_{\max} for the case of Langevin bimolecular recombination at various light absorption profiles (αd) and light intensities (L), demonstrating the strong experimental parameter-dependent shape of CELIV extraction current transients. Star symbols in panel (a) mark the extraction maximum current density Δj_{\max} and time t_{\max} .

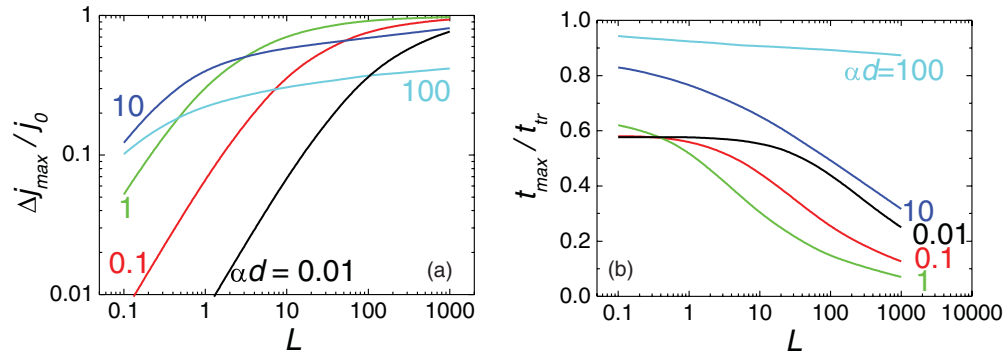


FIG. 2. (Color online) Numerically calculated and normalized maxima of extraction current density $\Delta j_{\max}/j_0$ (a) and extraction time t_{\max}/t_{tr} (b) shown for various light absorption profiles (αd). Note that, even at the highest carrier concentrations ($L > 1$), Δj_{\max} does not exceed the j_0 value ($\Delta j_{\max}/j_0 \leq 1$) due to Langevin bimolecular carrier recombination.

From the same numerically calculated CELIV current density transients, Δj_{\max} and t_{\max} were estimated at various L and αd , as shown in Figs. 2(a) and 2(b).

As can be seen from Fig. 2(a), the ratio of $\Delta j_{\max}/j_0$ follows a linear dependence at low photogenerated carrier concentrations and saturates to unity at the highest concentrations. The saturation can be explained in a similar manner to the standard Time-of-Flight (TOF) technique, where the recombination of the photogenerated charge carriers in the reservoir competes with carrier extraction.¹⁶ The extracted charge, and therefore the extraction current density, will saturate at high intensities because the bimolecular carrier lifetime becomes very short at high carrier concentrations. The fact that $\Delta j_{\max}/j_0 \leq 1$ can be conveniently used to experimentally determine the presence of Langevin bimolecular recombination at high light intensities confirms that CELIV, compared with TOF, is experimentally advantageous for determining the extent of Langevin bimolecular recombination because the interpretation of TOF results is not straightforward (in many cases misleading) for experimental cases where the extracted charge exceeds the CU limit (C is the device capacitance, and U is the applied external voltage), even in the case of Langevin recombination.⁶

Figure 2(b) shows numerically calculated t_{\max} as a function of photogenerated carrier concentration (L) at various light absorption profiles (αd). A weaker dependence of t_{\max} on L is observed for surface compared with volume photogeneration (αd large vs. small). This means that in thick films, where surface photogeneration is present, the error for estimating concentration-dependent carrier mobility is smaller. Similarly, in the case of volume photogeneration and low-to-moderate carrier concentrations, the carrier mobility is seen to be also weakly dependent on L .

To correctly calculate the mobility of photogenerated carriers using Eq. (2), t_{tr} must be corrected using experimentally measured t_{\max} at various L , as seen from Fig. 2(b). It is experimentally difficult to estimate L precisely, but by combining Fig. 2(a) and 2(b), t_{\max} can be replotted as a function of Δj_{\max} , as shown in Fig. 3. This approach allows the carrier concentration to be conveniently estimated from CELIV transients directly in the case of Langevin bimolecular recombination. Analytical solutions of t_{\max} at low carrier concentrations shown in Eq. (8) match very well with numerically calculated curves.

The final equation for carrier mobility calculation at various light absorption profiles and light intensities is written as:

$$\mu = K^2 \frac{2d^2}{At_{\max}^2}, \quad (9)$$

where $K = t_{\max}/t_{\text{tr}}$ is the correction factor. As can be seen from Fig. 3, the values of t_{\max}/t_{tr} at low concentrations of extracted carriers ($\Delta j_{\max} < j_0$) vary from $1/\sqrt{3}$ to 1, depending on αd , which exactly matches the coefficient in the analytical solution derived in the past.⁹

These results present the case of photogenerated carrier extraction, but for comparison, the correction factor, previously derived for equilibrium carrier extraction from the bulk of the film at intermediate equilibrium carrier concentrations¹⁰ is

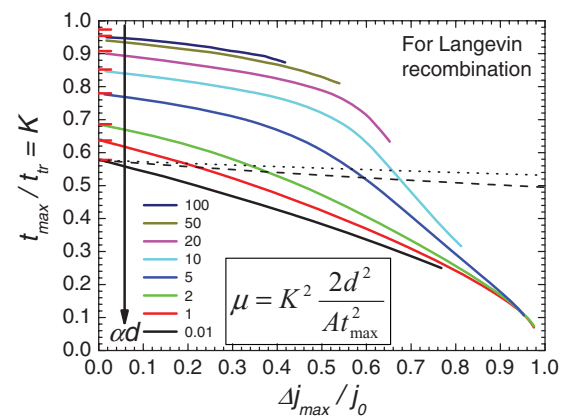


FIG. 3. (Color online) Numerically calculated extraction maximum time t_{\max} shown as a function of extracted carrier concentration, which is expressed as the ratio between Δj_{\max} and j_0 . The Langevin bimolecular carrier recombination case is analyzed. Different curves represent various light absorption profiles (αd). The correction factor $K = t_{\max}/t_{\text{tr}}$ is used to calculate the charge carrier mobility using Eq. (9) at given experimental conditions. Red hashes along the vertical axis show values calculated according to Eq. (8). The dashed line marks the case of equilibrium carrier extraction in the dark from the bulk of the film according to Eq. (10),¹⁰ whereas the dotted line presents the same equation but with a slightly different coefficient taken from Ref. 4.

shown in Fig. 3 as a dashed line. In this case carrier mobility is calculated using the expression

$$\mu = \frac{2d^2}{3At_{\max}^2(1 + 0.36\Delta j/j_0)}, \quad (10)$$

which cannot be used for photogenerated carrier extraction at various αd .

It has been previously demonstrated that the coefficient (0.36) in Eq. (10) might be slightly different;^{4,5} however, as one can see from Fig. 3 (dotted line compared with dashed line) the difference is negligible. From this analysis, we can see that it is crucially important to distinguish between equilibrium carrier extraction in the dark from the bulk of the film [Eq. (10)] and the photogenerated carrier extraction [Eq. (9)].

IV. EXPERIMENTAL RESULTS

To demonstrate that the above numerical calculations are relevant to the experiment, we have measured CELIV current transients at various laser intensities in phenyl-C61-butyric acid methyl ester (PCBM) thin films—the archetypal n-type fullerene acceptor used in organic solar cells. In this system, both Langevin and non-Langevin carrier recombination have been observed, depending on the efficiency of the solar cell.^{11–14} It is important to note that Langevin-type recombination is expected in low-mobility materials, such as polymers or disordered organic semiconductors.^{15–17} PCBM was chosen because it is a well-studied material with carrier mobility values ranging from 10^{-3} cm^2/Vs in diodes to 0.1 cm^2/Vs in organic field effect transistors at orders of magnitude higher carrier concentrations.^{18,19} We note that, in CELIV experiments, high charge carrier concentrations cannot be reached to match the carrier concentration in the channel of the field effect transistor. This results in lower carrier mobilities typically observed in CELIV and other diode-type structures fabricated from disordered organic semiconductors.²⁰

The device fabrication was performed in a nitrogen atmosphere, where PCBM was dissolved in chlorobenzene solution and spin cast on top of a pre-prepared indium tin oxide (ITO) substrate coated with a thin poly(3,4-ethylenedioxythiophene)-poly(styrenesulfonate) (PEDOT-PSS) film forming a sandwich-type device. As the top electrode, a thin semitransparent (20–30 nm) aluminum film was evaporated. By controlling the spin speed, the sample thickness was chosen such that the light absorption profile times film thickness would be $\alpha d = 5$ in the range where the shift in t_{\max} is strongest. Further description of the CELIV experimental setup and film preparation can be found elsewhere.¹²

In Fig. 4, CELIV current transients [Fig. 4(a)] at different laser intensities and carrier mobilities [Fig. 4(b)] calculated using Eqs. (9) and (10) are shown. Current transients resemble the calculated ones shown in Fig. 1; however, due to dispersive transport typically observed in organic semiconductors,³ the exact shape is slightly different. The Δj_{\max} saturates at high light intensities (inset of Fig. 4(b)) and $\Delta j_{\max} < j_0$. As seen from Fig. 1(a), this directly confirms the presence of Langevin recombination in PCBM and demonstrates the additional utility of the methodology.

As expected, the extraction maxima shift to shorter times at higher laser intensities (high carrier concentrations). Therefore, to correctly calculate the charge carrier mobility, Eq. (9) with correction factor K as shown in Fig. 3 was used. The estimated mobility values are seen to be different, demonstrating that the correction factor is required when estimating carrier mobility as a function of carrier concentration. Weak carrier-concentration-dependent carrier mobility is typically observed at low carrier concentrations (in diodes), since space-charge-limited current condition limits the carrier concentration to values two orders of magnitude lower compared with what is usually measured in the channel of field effect transistors.

It is also worth stating that, as has been previously shown, CELIV current transients are also influenced by trapped

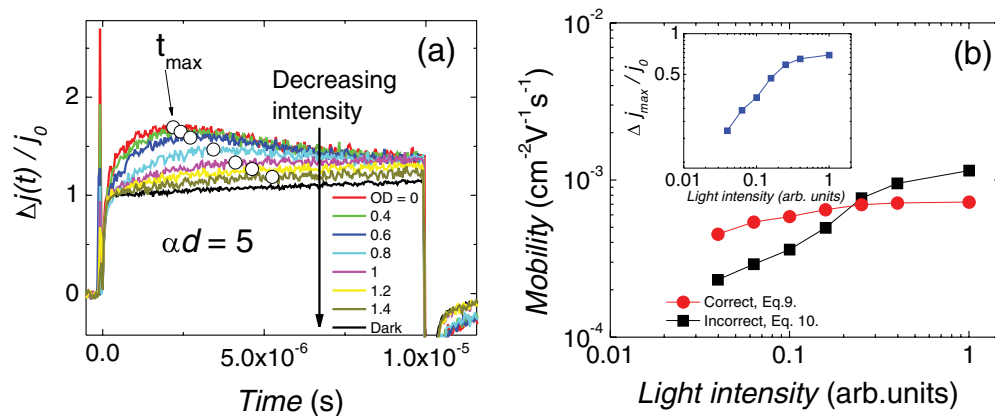


FIG. 4. (Color online) (a) Experimental CELIV current transients in PCBM films acquired at various light intensities using neutral-density filters of increasing optical density (OD). Open circles mark the position of the extraction maxima from which carrier mobilities are calculated (b). Mobilities of photogenerated carriers are calculated using either Eq. (9) with a correction factor (red [gray] circles) or Eq. (10) for equilibrium mobility calculation (black squares), which must be used for equilibrium carrier extraction. Inset shows the saturation of extraction maximum current density (Δj_{\max}) at high light intensities to values lower than the displacement current density (j_0), proving Langevin bimolecular carrier recombination.

carriers, which redistribute the applied electric field.²¹ However, in the case presented here, we did not observe any dependence of the current transients on the repetition rate of the applied voltage pulses. Hence, we can safely neglect the effects of carrier trapping.

V. CONCLUSIONS

In conclusion, analytical CELIV equations describing extraction current transients and extraction maximum times at low carrier concentrations and various light absorption profiles are derived. Numerical calculations in strong agreement with these analytical expressions demonstrate that the extraction maximum current cannot exceed the displacement current in the case of Langevin bimolecular carrier recombination. This can be conveniently used to test for the type of bimolecular recombination at high light intensities. Numerical calculations and experimental results demonstrate strong shifts in extraction maximum times of CELIV current

transients when Langevin bimolecular carrier recombination is present. Finally, a universal procedure to calculate charge carrier mobility using the appropriate correction factor at various photogenerated carrier concentrations and light absorption profiles is presented. This methodology significantly extends the utility of CELIV as a technique for charge transport analysis in a wide range of disordered semiconductors.

ACKNOWLEDGMENTS

Financial support from the Research Council of Lithuania through Project No. VP1-3.1-ŠMM-07-K-01-023 is acknowledged. The Centre for Organic Photonics and Electronics is a strategic initiative funded by the University of Queensland. Paul Meredith acknowledges the support of the Queensland Government through the award of a Smart State Senior Fellowship and the University of Queensland through a Vice Chancellors Senior Research Fellowship Award.

*almantas.pivrikas@gmail.com

¹A. J. Mozer, N. S. Sariciftci, A. Pivrikas, R. Österbacka, G. Juška, L. Brassat, and H. Bässler, *Phys. Rev. B* **71**, 035214 (2005).

²C. Deibel, A. Baumann, and V. Dyakonov, *Appl. Phys. Lett.* **93**, 163303 (2008).

³R. Österbacka, A. Pivrikas, G. Juška, K. Genevičius, K. Arlauskas, and H. Stubb, *Current Applied Physics* **4**, 534 (2004).

⁴S. Bange, M. Schubert, and D. Neher, *Phys. Rev. B* **81**, 035209 (2010).

⁵J. Lorrmann, B. H. Badada, O. Inganäs, V. Dyakonov, and C. Deibel, *J. Appl. Phys.* **108**, 113705 (2010).

⁶G. Juška, M. Viliūnas, O. Klima, E. Šipek, and J. Kočka, *Phil. Mag. B* **69**, 277 (1994).

⁷G. Juška, M. Viliūnas, K. Arlauskas, and J. Kočka, *Phys. Rev. B* **51**, 16668 (1995).

⁸A. Petravičius, G. Juška, and R. Baubinas, *Sov. Phys. Semicond.* **9**, 1530 (1975).

⁹G. Juška, K. Arlauskas, M. Viliūnas, and J. Kočka, *Phys. Rev. Lett.* **84**, 4946 (2000).

¹⁰G. Juška, K. Arlauskas, M. Viliūnas, K. Genevičius, R. Österbacka, and H. Stubb, *Phys. Rev. B* **62**, R16235 (2000).

¹¹A. Pivrikas, H. Neugebauer, and N. S. Sariciftci, *IEEE J. Sel. Top. Quantum Electron.* **16**, 1746 (2010).

¹²R. Osterbacka, A. Pivrikas, G. Juska, A. Poskus, H. Aarnio, G. Sliuzys, K. Genevicius, K. Arlauskas, and N. S. Sariciftci, *IEEE J. Sel. Top. Quantum Electron.* **16**, 1738 (2010).

¹³A. Pivrikas, N. S. Sariciftci, G. Juška, and R. Österbacka, *Progress in Photovoltaics: Research and Applications Special Issue: Organic Solar Cells* **15**, 677 (2007).

¹⁴G. Juska, K. Genevicius, G. Sliuzys, A. Pivrikas, M. Scharber, and R. Osterbacka, *J. Appl. Phys.* **101**, 114505 (2007).

¹⁵M. Pope and C. E. Swenberg, *Electronic Processes in Organic Crystals and Polymers*, 2nd ed. (Oxford University Press, New York, 1999).

¹⁶A. Pivrikas, G. Juška, R. Österbacka, M. Westerling, M. Viliūnas, K. Arlauskas, and H. Stubb, *Phys. Rev. B* **71**, 125205 (2005).

¹⁷A. Pivrikas, R. Osterbacka, G. Juska, K. Arlauskas, and H. Stubb, *Synth. Met.* **155**, 242 (2005).

¹⁸V. D. Mihailetschi, J. K. J. van Duren, P. W. M. Blom, J. C. Hummelen, R. A. J. Janssen, J. M. Kroon, M. T. Rispens, W. J. H. Verhees, and M. M. Wienk, *Adv. Func. Matter.* **13**, 43 (2003).

¹⁹T. D. Anthopoulos, D. M. de Leeuw, E. Cantatore, S. Setayesh, E. J. Meijer, C. Tanase, J. C. Hummelen, and P. W. M. Blom, *Appl. Phys. Lett.* **85**, 4205 (2004).

²⁰A. Pivrikas, M. Ullah, T. B. Singh, C. Simbrunner, G. Matt, H. Sitter, and N. S. Sariciftci, *Organic Electronics* **12**, 161 (2011).

²¹G. Juška, M. Viliūnas, K. Arlauskas, N. Nekrašas, N. Wyrsh, and L. Feitknecht, *J. Appl. Phys.* **89**, 4971 (2001).